

String-like theory as solution to the sign problem of a finite density gauge theory

Kurt Langfeld*

Department of Mathematical Sciences, University of Liverpool, UK

E-mail: kurt.langfeld@liverpool.ac.uk

Z₃ gauge theory with dynamical (bosonic) matter is studied in 4 dimensions with a finite chemical potential. This theory could be viewed as an effective theory describing the centre vortex picture of QCD colour confinement, but it is studied here with local interactions as theory in its own right. It is shown that the sign-problem can be solved by dualisation. The dual theory is derived: the pure gauge sector is a theory of closed membranes with Nambu-Goto action, and matter is described by open branes bounded by closed matter loops. The brane theory is simulated with Monte-Carlo techniques. Some evidence is found that the theory possesses a weakly-renormalisable phase with the scale set by a mass gap. Deconfinement at low temperatures and finite chemical potentials appears as a percolation transition for matter loops.

*XIII Quark Confinement and the Hadron Spectrum - Confinement2018
31 July - 6 August 2018
Maynooth University, Ireland*

*Speaker.

1. Introduction

The phasediagram of strongly interacting matter (as a function of the temperature T and the chemical potential μ) is believed to be informed by the transition from colour-confined to deconfined matter. However, our current understanding of this transition is derived from effective considerations and model building that usually know little about quark confinement. I give two examples: to reconcile large N -arguments with an effective quark model description led to the postulate of a so-called quarkyonic phase [1] and, secondly, effective quark models could justify the existence of “chiral spirals” or “Fermi-Einstein condensation” [2, 3].

By contrast, first principle lattice gauge simulations have shed light on the QCD confinement mechanism for a vanishing chemical potential. It started with the discovery of a linear-rising potential between static quark sources induced by a colour-electric flux tube forming between the sources [4]. It remained to clarify why QCD electric flux tends to squeeze into tubes as opposed to the case of flux spreading out in QED. A possible explanation was offered twenty years ago by Del Debbio, Faber, Greensite and Olejnik: after gauge fixing, the projection of the $SU(N)$ gauge field configurations to those taking values in the centre Z_N of the group produces a theory that retains colour confinement [5, 6, 7]. Further significance was added by the discovery that the Z_N gauge invariant degrees of freedom, the so-called centre-vortices, have properties dictated by the physical mass scale and survive in the continuum limit [8]. A decade long fruitful discussion followed which revealed the vortex signature in the high temperature deconfinement transition [9, 10] or for chiral symmetry breaking [11, 12], and investigations of the vortex confinement mechanism extended to gauge groups without a centre [13]. However, very little is known about the centre vortex properties for light quark masses, let alone for finite density QCD.

Rather than adding to the extensive literature of effective descriptions of the QCD phase diagram, I here would like to rise the question: Can we deform QCD to a theory that still has linear colour confinement and, at the same time, admits a first principle calculation of its phase diagram?

I will show that Z_3 gauge theory with bosonic matter in four dimensions is an answer. At finite chemical potentials for the Z_3 matter, direct Monte-Carlo simulations are ruled out by a strong sign-problem. The recent years have seen remarkable advances for simulating those theories: Complexification of fields [14] gave rise to Complex Langevin simulations [15, 16] or Lefschetz Thimble inspired methods [17]. Algorithmic advances [18] may generically give reliable results for medium size systems (e.g. [19, 20]). A powerful method for solving sign problems is dualisation [21, 22]: a transformation of field variables on the dual lattice may or may not produce a real theory upon the integration of the original variables. This frequently leads to non-local degrees of freedom sometimes called “worms” or flux-lines [23].

2. Brane theory from Z_3 gauge theory with Z_3 matter

2.1 The model

Let us consider a 4-dimensional hyper-cubic lattice of extent $N^3 \times N_t$ and periodic boundary conditions. The protagonists of the lattice simulation are Z_3 group elements associated with the

links of the lattice (“Gluon” fields) and with the sites (“matter” field):

$$U_\mu(x), \sigma(x) \in \{1, z, z^\dagger\}, \quad z = \exp\left\{i\frac{2\pi}{3}\right\}. \quad (2.1)$$

The partition function Z of the theory features both, a pure gluonic action and an interaction term:

$$Z = \sum_{\sigma, U_\mu} \exp\{S_g[U] + S_f[\sigma, U]\}, \quad (2.2)$$

$$S_g[U] = 2\beta \sum_p \operatorname{Re} P_p, \quad P_{p=(x, \mu < \nu)} = U_\mu(x) U_\nu(x + \mu) U_\mu^\dagger(x + \nu) U_\nu^\dagger(x), \quad (2.3)$$

$$S_f[\sigma, U] = 2\kappa \sum_{x, \mu=1\dots 3} \operatorname{Re} \left[\sigma^\dagger(x) U_\mu(x) \sigma(x + \mu) \right] \quad (2.4)$$

$$+ 2\kappa \sum_{x, \mu=4} \left[e^\mu \sigma^\dagger(x) U_\mu(x) \sigma(x + \mu) + e^{-\mu} \sigma^\dagger(x) U_\mu^\dagger(x - \mu) \sigma(x - \mu) \right],$$

where p specifies an elementary plaquette of the lattice.

2.2 Dualisation

We are now going to sum over the fields $U_\mu, \sigma \in Z_3$. I will only outline the calculation disregarding the matter fields by setting $\kappa = 0$. Further details will be presented in a forthcoming publication. The Z_3 algebra greatly facilitates this calculation:

$$U \in Z_3: \quad U^3 = 1, \quad UU^\dagger = 1, \quad \sum_{U \in Z_3} U = 0. \quad (2.5)$$

Because of these properties, we find for any bivariate function f , which admits a Taylor expansion in both of its arguments:

$$f(U, U^\dagger) = a + bU + cU^\dagger,$$

where a, b, c are numerical constants. In particular, the “gluonic” Gibbs factor can hence be written as:

$$\exp\{S_g\} = \prod_p \exp\left[\beta(P_p + P_p^\dagger)\right] = \prod_p c(\beta) \left[1 + t(\beta)(P_p + P_p^\dagger)\right]. \quad (2.6)$$

$$c(\beta) = \frac{1}{3} e^{2\beta} + \frac{2}{3} e^{-\beta}, \quad t(\beta) = \frac{e^{2\beta} - e^{-\beta}}{e^{2\beta} + 2e^{-\beta}}. \quad (2.7)$$

Note that, for the interesting regime $\beta > 0$, $t(\beta)$ is positive.

The next step is to expand the brackets in (2.6) of the product. For this purpose, we introduce auxiliary variables n_p (one for each plaquette p), which later become the degrees of freedom that span the membrane:

$$\mathbb{1} + tP_p + tP_p^\dagger = \sum_{n_p=-1,0,1} \left[\delta_{n_p,0} \mathbb{1} + \delta_{n_p,1} tP_p + \delta_{n_p,-1} tP_p^\dagger \right] = \sum_{n_p=-1,0,1} t^{|n_p|} P^{n_p}.$$

The gluonic Gibbs factor (2.6) is then given by (with $V = N^3 \times N_t$ the lattice size):

$$\exp\{S_g\} = c(\beta)^{6V} \sum_{\{n_p\}} \prod_p t(\beta)^{|n_p|} P^{n_p}. \quad (2.8)$$

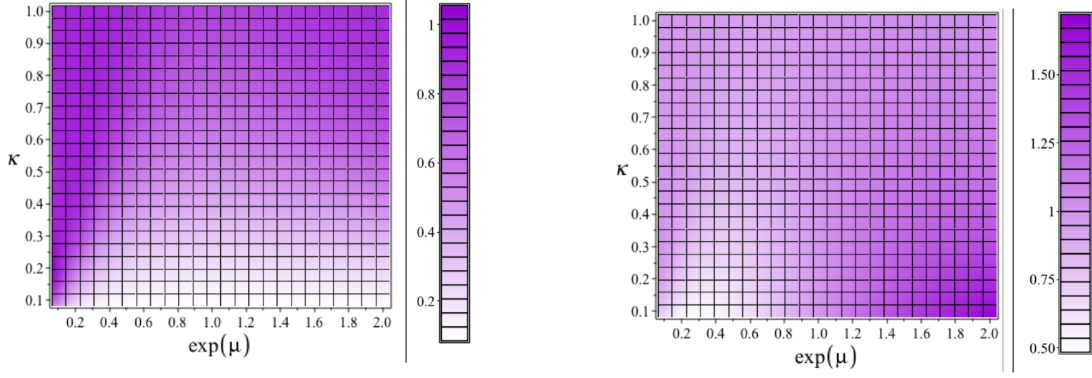


Figure 1: The emerging functions t_f and Ω for a selected range of the hopping parameter κ and the fugacity $\exp\mu$.

We have now a plaquette field n_p at our finger tips: a n_p -configuration has a value 0,1 or -1 for each plaquette. If we find $n_p = 0$ for a given plaquette p , we say it is “trivial”, i.e., it does not contribute to the factor in (2.8). We are now in the position to sum over all link fields and to rewrite the partition function in terms of the new plaquette field (recall $\kappa = 0$):

$$Z_g = c(\beta)^{6V} \sum_{\{n_p\}} \sum_{\{U_\mu\}} \prod_P t(\beta)^{|n_p|} P^{n_p}.$$

Depending on the plaquette configuration, P^{n_p} is a product of many link fields. Due to the property (2.5), many of this products vanish upon summation over the Z_3 elements, e.g., if a particular link U_ℓ of a non-trivial plaquette p stands alone. Another example is if two neighbouring non-trivial plaquettes contribute each a factor U_ℓ , we would find: $\sum U_\ell^2 = 0$. A way to avoid producing a vanishing contribution to the partition function is the following: the non-trivial plaquettes only contribute links U_ℓ and U_ℓ^\dagger at the same time and we would find $\sum U_\ell U_\ell^\dagger = 3$. We now see that the summation over the Z_3 elements introduces constraints to set of plaquette values $\{n_p\}$, and we introduce

$$\sum_{\{U_\mu\}} \prod_P P^{n_p} =: 3^{4V} \delta_{\text{closed}}(\{n_p\}), \quad (2.9)$$

where $\delta_{\text{closed}}(\{n_p\}) = 1$ if the constraints are satisfied and vanishes in all other cases. I will now argue that if the n_p of a configuration $\{n_p\}$ form a set of closed oriented surfaces, the constraint is satisfied. To this aim, let c denote an elementary cube of the lattice, and let $p \in c$ denote all plaquettes forming the surface of the cube (the plaquette contribute a P_p pr P_p^\dagger depending on the position on the surface). The Z_3 Bianchi identity then yields:

$$\prod_{p \in c} P_p[U_{\ell \in p}] = 1.$$

Note that if a set of cubes has a plaquette p in common, we can set $n_p = 0$ since the plaquettes come in pairs P and P^\dagger . Hence, if the set of n_p form arbitrary but closed surfaces, we would find $\delta_{\text{closed}}(\{n_p\}) = 1$. Altogether, we find:

$$Z_g = c(\beta)^{6V} 3^{4V} \sum_{\{n_p\}} \prod_P t(\beta)^{|n_p|} \delta_{\text{closed}}(\{n_p\}) = c(\beta)^{6V} 3^{4V} \sum_{\{n_p\}, \text{closed}} \prod_P t(\beta)^{|n_p|} \quad (2.10)$$

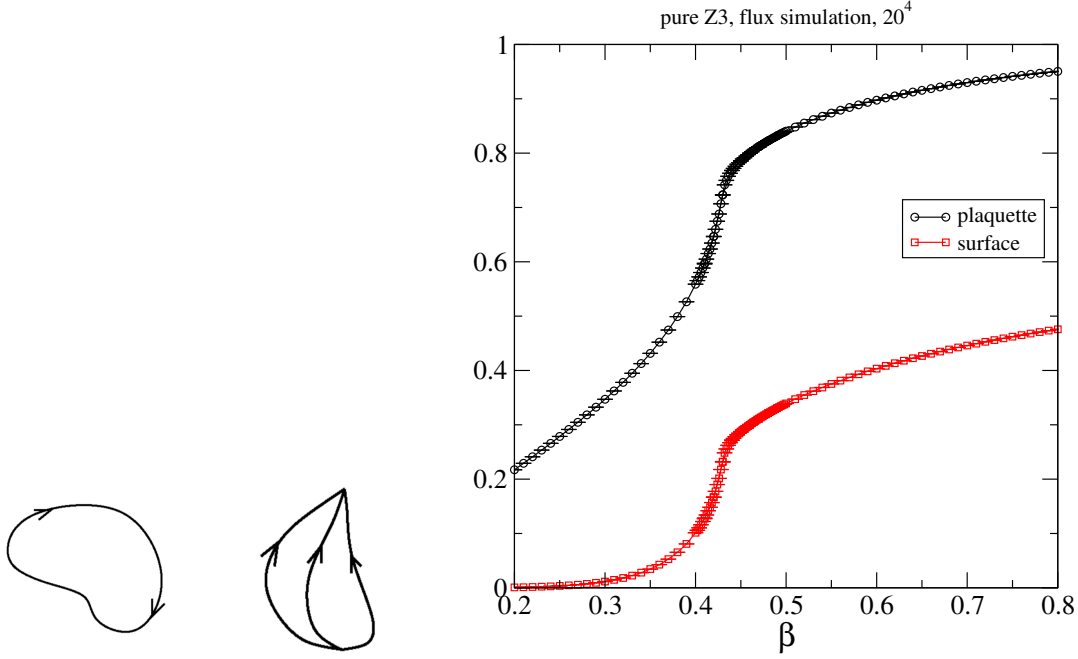


Figure 2: Left: Allowed flux lines configurations: "mesonic" type (left) and "baryonic" type (right). Right: Average plaquette and the fraction of the 2-brane surface area as a function of β .

Defining the area A of the closed surfaces and the "surface tension" τ by,

$$A[\{n_p\}] = \sum_p |n_p|, \quad \tau := -\ln t(\beta),$$

The gluonic partion function can be viewed as a theory of closed membranes with a Nambu-Goto action:

$$Z_g = c(\beta)^{6V} 3^{4V} \sum_{\{n_p\}, \text{closed}} \exp[-\tau A[\{n_p\}]]. \quad (2.11)$$

We now need to include the matter fields. The derivation follows the lines above and starts with a character expansion of the Gibbs factor. It starts noting that (for a given link $\ell = (x\mu)$) $K_\ell = \sigma^\dagger(x)U_\mu(x)\sigma(x)$ is an element of the group Z_3 , and thus

$$\exp\{S_f\} = \prod_\ell c_f(\kappa, \mu) \left\{ \mathbb{1} + t_f(\kappa, \mu) \left[\Omega(\kappa, \mu) K_\ell + \frac{1}{\Omega(\kappa, \mu)} K_\ell^\dagger \right] \right\}, \quad (2.12)$$

where a c_f , t_f and Ω can be readily calculated. The result is lengthy and will be presented elsewhere. I just point out that for $\mu = 0$, the action S_f (2.4) is real, and we have $\Omega(\kappa, 0) = 1$. For the emerging string-like theory, it will be important that t_f and Ω are positive. A phenomenological relevant range is $\kappa = 0.1 \dots 1$ and $\exp\mu = 0.1 \dots 2$. The colour plot in figure 1 shows that both, t_f and Ω , are indeed positive within safe margins.

To expand the brackets in (2.12), we introduce for each link ℓ a flux variable k_ℓ by

$$\mathbb{1} + \Omega(\kappa, \mu) K_\ell + \frac{1}{\Omega(\kappa, \mu)} K_\ell^\dagger = \sum_{k_\ell=-1,0,1} \left[\delta_{k_\ell,0} \mathbb{1} + \delta_{k_\ell,1} t_f \Omega K_\ell + \delta_{k_\ell,-1} \frac{t_f}{\Omega} K_\ell \right].$$

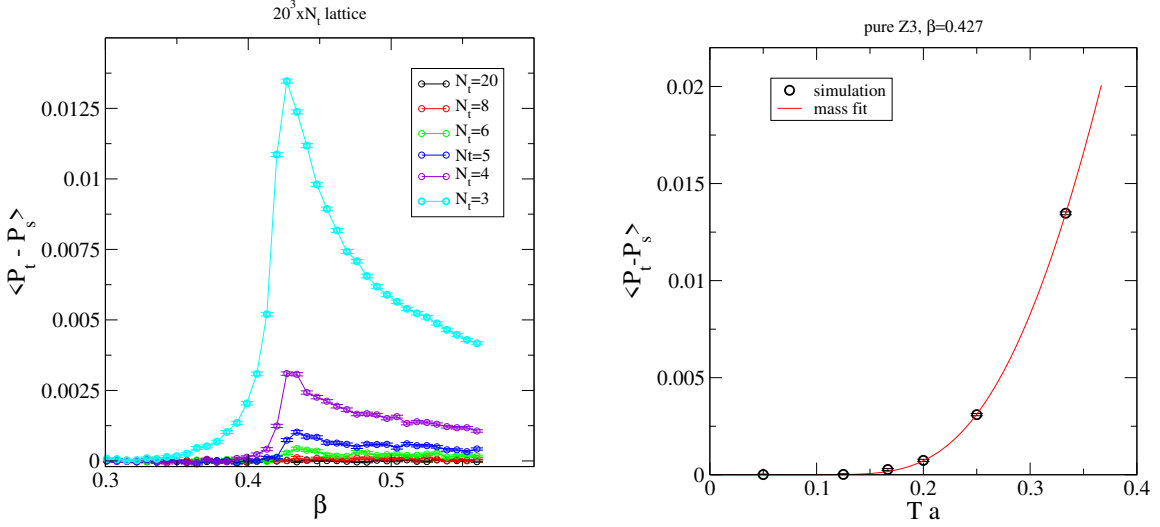


Figure 3: Left: Difference of time-like and space-like plaquettes on a $N^3 \times N_t$ asymmetric lattice as a function of β . Right: The difference for $\beta = 0.427$ as a function of the temperature $Ta = 1/N_t$.

This turns (2.12) into:

$$\exp\{S_f\} = c_f^{4V} \sum_{\{k_\ell\}} \prod_{\ell} t_f^{|k_\ell|} [\Omega K_\ell]^{k_\ell}. \quad (2.13)$$

The final step is to “integrate out” the gauge fields U_μ and the matter fields σ . Inserting (2.8) and (2.12) into the partition function (2.2), the summation over the original fields produces an equivalent formulation of the partition function in terms of the plaquette variables n_p and the flux variables k_ℓ :

$$Z(\beta, \kappa, \mu) = 3^{7V} c(\beta)^{6V} c_f(\kappa, \mu)^{4V} \sum_{\{n_p, k_\ell\}, \text{closed}} t^{A(n_p)} t_f^{L(k_\ell)} \Omega^{t_+(k_\ell) - t_-(k_\ell)}, \quad (2.14)$$

where the constraints on the sets for n_p and k_ℓ are as follows:

- The set of oriented flux variables k_ℓ form closed lines that either form a loop or start (and end) in points of multiple of 3 (see figure 2 for an illustration).
- The set of oriented plaquette variables n_p form either closed surfaces or open surfaces that are bounded by flux loops.

Furthermore, $A(n_p)$ is the total “gluonic” surface area, i.e., the number of non-trivial plaquettes $\sum_p |n_p|$. The total length of the flux lines is denoted $L(k_\ell)$, and $t_+(k_\ell)$ is the number of flux in positive time direction and $t_-(k_\ell)$ the sum of those timelike fluxes that are oriented in negative time direction.

3. Brane theory - pure Z3 gauge theory

In order to carry out a simulation of the brane theory (2.11), we need to create configurations with closed surfaces. I am using a standard Metropolis update that visits elementary cubes on the

lattice and deforms the existing configuration of closed surfaces by adding and removing plaquettes of the surface according to the orientation of the cube's plaquette. This guarantees the MC update does not violate the constraints. The underlying assumption is that this MC update is ergodic, i.e., that it can generate *all* sets n_p compatible with $\delta_{closed} \neq 0$ in (2.9). At the current stage, the numerical approach generating the specific sets of configuration should be viewed as definition of the model until a rigorous link between the MC approach and the Z3 theory is established.

As a first observable, I study the average plaquette

$$\frac{1}{2} \frac{1}{6V} \frac{\partial \ln Z_g}{\partial \beta} = \frac{1}{2} \frac{\partial \ln c(\beta)}{\partial \beta} + \frac{1}{2} \frac{\partial \ln t(\beta)}{\partial \beta} \langle |n_p| \rangle, \quad (3.1)$$

where I have used (2.10). The fraction $\langle |n_p| \rangle$ of non-trivial surfaces on the lattice and the average plaquette are related by numerical constants. Both quantities are shown in Figure 2, right panel. In the strong coupling regime at small β , the 2-brane surfaces are suppressed and the β -dependence of the plaquette is dictated by the first term in (3.1). The transition from the strong coupling regime to saturation at high β (sometimes called “roughening transition”) is seen in the brane theory as the onset when the brane surfaces start populating the empty vacuum.

Temperature, say T , in quantum field theory is usually introduced by the extent of the torus in time direction:

$$\frac{1}{T} = N_t a \quad a : \text{lattice spacing.}$$

Renormalisation on the lattice is usually performed by demanding that a physical mass m does not change under a change of the lattice regulator a . Measuring the scaling function $s(\beta)$ then defines the lattice spacing as a function of the bare coupling parameter β :

$$ma = s(\beta) \quad \Rightarrow \quad a(\beta) = \frac{s(\beta)}{m},$$

where m plays the role of the free parameter (rather than the coupling strength) and serves as a reference scale. A correlation length (i.e., the inverse mass gap) is most easily detected on asymmetric lattices using an observables that detects lattice asymmetries. A possibility is the difference between time-like and space-like plaquette averages, i.e., $\langle P_t - P_s \rangle$, which informs the entropy density in Yang-Mills theories. As soon as the correlation length is large enough to equal the (smaller) time-like extent $N_t a$ of the lattice, $\langle P_t - P_s \rangle$ will be significantly different from zero. Figure 3 shows the difference as a function of β for several sizes N_t . The data show a clear peak around $\beta \approx 0.43$, which is more pronounced for a small temporal extent. The right panel of the same graph shows the difference for several temperatures at a fixed value of β . If the theory possesses a mass gap m , thermal excitations of the lightest excitation would imply:

$$\langle P_t - P_s \rangle \propto \exp\left\{-\frac{m}{T}\right\} = \exp\left\{-\frac{ma}{Ta}\right\}.$$

Indeed, the data are very well fitted by this ansatz (see red line if figure 3). Repeating this analysis for several values for β determines the lattice spacing in terms of the mass gap m :

β	0.413	0.420	0.427	0.434
$ma(\beta)$	2.503(1)	2.163(5)	1.463(1)	1.346(1)

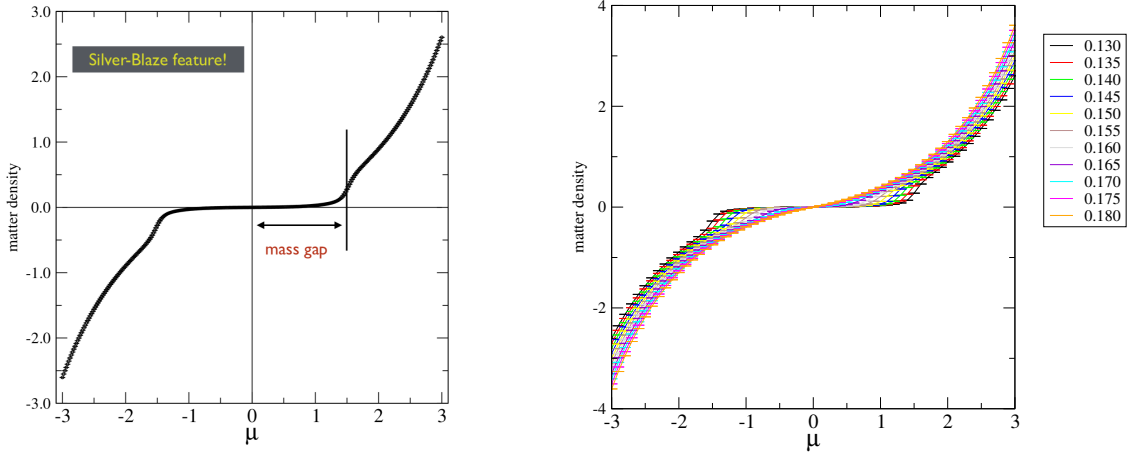


Figure 4: Left: Matter density as a function of the chemical potential for $\beta = 0.43$ and $\kappa = 0.130$ and a 20^4 lattice. Right: Same as left but for several values of κ .

We see a UV type scaling: the lattice spacing a shrinks with increasing β . It is expected that the Z3 gauge theory possesses a first order phase transition: the correlation length stays finite, and a continuum limit $a \rightarrow 0$ does not exist. However, the model could be *weakly renormalisable*: the infrared physics of the theory is largely insensitive to the regulator for $a > a_{\text{critical}}$. A famous example of such a weakly renormalisable theory is QED. Another quite recent example is from Philipsen and collaborators: they have started to study lattice QCD for rather coarse lattices using the strong coupling expansion and manage to extract rather robust infrared results (see e.g. [24]).

4. Branes, matter loops and finite densities

We now consider the full Z3 gauge theory with dynamical matter at the presence of a finite chemical potential μ . As explained above, the dual theory is a theory of closed and open branes bounded by matter loops. The surface tension is informed by $t(\beta)$ and the string tension of the matter loops by $t_f(\kappa, \mu)$ and $\Omega(\kappa, \mu)$. The “normalisation” constants c and c_F also depend on the theory parameters:

$$Z(\beta, \kappa, \mu) = 3^{N_\ell + V} c(\beta)^{N_p} c_f(\kappa, \mu)^{N_\ell} \sum_{n_p, k_\ell} t^{S(n_p, k_\ell)} t_f^{L(k_\ell)} \Omega^{t_+(k_\ell) - t_-(k_\ell)}$$

$\uparrow \qquad \qquad \qquad \uparrow \qquad \qquad \qquad \uparrow$
 μ dependence

Note that the matter density

$$\rho(\mu) = \frac{d \ln Z}{d \mu}$$

receives several contributions from the string theory variables:

$$\rho(\mu) = N_\ell \frac{d \ln c_f}{d \mu} + \frac{d \ln t_f}{d \mu} \langle L(k_\ell) \rangle + \frac{d \ln \Omega}{d \mu} \langle t_+(k_\ell) - t_-(k_\ell) \rangle. \quad (4.1)$$

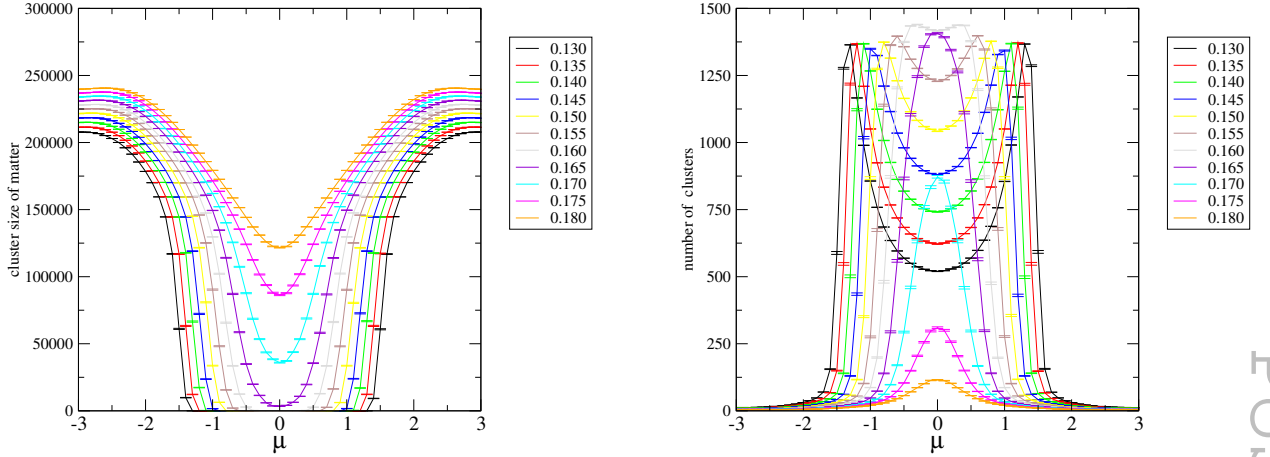


Figure 5: Left: Average size of matter clusters as a function of the chemical potential. Right: average number of clusters populating the lattice.

It is expected that for a chemical potential smaller than the matter mass gap, $\mu < m_f$, the density remains zero in the infinite volume limit (“Silverblaze” feature). We stress that this is highly non-trivial in the string theory formulation and involves intricate cancellations in (4.1). At medium size chemical potentials, the term on the far right of (4.1) strongly contributes to the density. Note that closed matter loops, i.e., the “mesonic” loops, have $t_+(k_\ell) - t_-(k_\ell)$ and that only the “baryonic” loop configuration (see figure 2, left panel) do contribute.

We have simulated the full (brane) theory using a simple Metropolis update. The elementary move for updating the closed “gluon” surfaces is “adding an elementary cube with oriented surfaces”. Two elementary moves are necessary to update the open surfaces bound by matter loops: A “mesonic” update adds the oriented loop around an elementary plaquette and the plaquette to the gluon surfaces; A “baryonic” update adding three matter lines part of a 1×2 rectangular surface. Changing the orientation of the surface or the flux then generates the “inverse” move needed for detailed balance. Details will be presented in a forthcoming publication.

Figure 4 shows our numerical findings for the density $\rho(\mu)$ as a function of the chemical potential μ for the case of rather large matter mass dictated by a hopping parameter $\kappa = 0.130$. We indeed observe the “silver blaze” feature: the density almost vanishes up to a certain threshold value μ_c when it rapidly increases. The small variations of the density for $\mu < \mu_c$ might be well explained by the finite lattice size. This interpretation is affirmed by reducing the matter mass, i.e., increasing κ and observing that μ_c decreases (see figure 4, right panel). For large enough $\kappa \gtrsim 0.165$, we observe an immediate response of the density to the presence of a chemical potential. We might interpret this value of κ as the massless case.

Let us explore further the properties of matter as a function of μ and several masses informed by κ . Figure 5, left panel, shows the average number of links that are connected to the other links of one cluster. Let us focus on $\mu = 0$: For large matter masses (e.g., $\kappa = 0.130$), we observe that

only few and small clusters are present. For $\kappa = 0.165$, which we defined as the massless limit above, we observe that the vacuum is populated by rather large clusters. Increasing κ further, we observe a proliferation of matter loops and, perhaps, a less interesting phase for phenomenological purposes.

If we now focus on the μ -dependence, we observe for large matter masses (e.g., $\kappa = 0.130$) that, at the onset chemical potential, a proliferation of large clusters sets in. At the same time, the average number of clusters sharply drops (see figure 5, right panel). These findings are compatible with the deconfinement mechanism put forward by Helmut Satz in the nineties [25]: at a critical baryon density, baryons start to overlap and the quarks can free percolate.

Note that there is also an important lesson to learn for QCD models: in the subcritical region $\mu < \mu_c$ in the “silverblaze region”, the properties of the (brane and loop) fields do significantly depend on the chemical potential. These properties then conspire and produce a cancellation of a μ -dependence in physical observables such as the density. This implies that effective models of QCD (such as constituent quark models) need not necessarily be independent from the chemical potential in the silverblaze regime.

Acknowledgements: I thank David Schaich and Radu Tatar for helpful comments, and, of course, the organisers for an excellent conference. The numerical simulations were carried out at the HPC facility Barkla at the University of Liverpool. Support is greatly acknowledged.

References

- [1] L. McLerran and R. D. Pisarski, Nucl. Phys. A **796** (2007) 83 doi:10.1016/j.nuclphysa.2007.08.013 [arXiv:0706.2191 [hep-ph]].
- [2] T. Kojo, Y. Hidaka, L. McLerran and R. D. Pisarski, Nucl. Phys. A **843** (2010) 37 doi:10.1016/j.nuclphysa.2010.05.053 [arXiv:0912.3800 [hep-ph]].
- [3] K. Langfeld and A. Wipf, Annals Phys. **327** (2012) 994 doi:10.1016/j.aop.2011.11.020 [arXiv:1109.0502 [hep-lat]].
- [4] F. Bissey, F. G. Cao, A. R. Kitson, A. I. Signal, D. B. Leinweber, B. G. Lasscock and A. G. Williams, Phys. Rev. D **76** (2007) 114512 doi:10.1103/PhysRevD.76.114512 [hep-lat/0606016].
- [5] L. Del Debbio, M. Faber, J. Greensite and S. Olejnik, Phys. Rev. D **55** (1997) 2298 doi:10.1103/PhysRevD.55.2298 [hep-lat/9610005].
- [6] L. Del Debbio, M. Faber, J. Giedt, J. Greensite and S. Olejnik, Phys. Rev. D **58** (1998) 094501 doi:10.1103/PhysRevD.58.094501 [hep-lat/9801027].
- [7] K. Langfeld, Phys. Rev. D **69** (2004) 014503 doi:10.1103/PhysRevD.69.014503 [hep-lat/0307030].
- [8] K. Langfeld, H. Reinhardt and O. Tennert, Phys. Lett. B **419** (1998) 317 doi:10.1016/S0370-2693(97)01435-4 [hep-lat/9710068].
- [9] M. Engelhardt, K. Langfeld, H. Reinhardt and O. Tennert, Phys. Rev. D **61** (2000) 054504 doi:10.1103/PhysRevD.61.054504 [hep-lat/9904004].
- [10] K. Langfeld, Phys. Rev. D **67** (2003) 111501 doi:10.1103/PhysRevD.67.111501 [hep-lat/0304012].

- [11] J. Gattnar, C. Gatttringer, K. Langfeld, H. Reinhardt, A. Schafer, S. Solbrig and T. Tok, Nucl. Phys. B **716** (2005) 105 doi:10.1016/j.nuclphysb.2005.03.027 [hep-lat/0412032].
- [12] P. O. Bowman, K. Langfeld, D. B. Leinweber, A. Sternbeck, L. von Smekal and A. G. Williams, Phys. Rev. D **84** (2011) 034501 doi:10.1103/PhysRevD.84.034501 [arXiv:1010.4624 [hep-lat]].
- [13] J. Greensite, K. Langfeld, S. Olejnik, H. Reinhardt and T. Tok, Phys. Rev. D **75** (2007) 034501 doi:10.1103/PhysRevD.75.034501 [hep-lat/0609050].
- [14] D. Sexty, PoS LATTICE **2014** (2014) 016 doi:10.22323/1.214.0016 [arXiv:1410.8813 [hep-lat]].
- [15] G. Aarts, F. A. James, J. M. Pawłowski, E. Seiler, D. Sexty and I. O. Stamatescu, JHEP **1303** (2013) 073 doi:10.1007/JHEP03(2013)073 [arXiv:1212.5231 [hep-lat]].
- [16] D. Sexty, J. Phys. Conf. Ser. **742** (2016) no.1, 012011. doi:10.1088/1742-6596/742/1/012011
- [17] A. Alexandru, G. Basar, P. F. Bedaque, G. W. Ridgway and N. C. Warrington, Phys. Rev. D **95** (2017) no.1, 014502 doi:10.1103/PhysRevD.95.014502 [arXiv:1609.01730 [hep-lat]].
- [18] K. Langfeld, PoS LATTICE **2016** (2017) 010 doi:10.22323/1.256.0010 [arXiv:1610.09856 [hep-lat]].
- [19] K. Langfeld and B. Lucini, Phys. Rev. D **90** (2014) no.9, 094502 doi:10.1103/PhysRevD.90.094502 [arXiv:1404.7187 [hep-lat]].
- [20] N. Garron and K. Langfeld, Eur. Phys. J. C **76** (2016) no.10, 569 doi:10.1140/epjc/s10052-016-4412-2 [arXiv:1605.02709 [hep-lat]].
- [21] M. G. Endres, Phys. Rev. D **75** (2007) 065012 doi:10.1103/PhysRevD.75.065012 [hep-lat/0610029].
- [22] C. Gatttringer and K. Langfeld, Int. J. Mod. Phys. A **31** (2016) no.22, 1643007 doi:10.1142/S0217751X16430077 [arXiv:1603.09517 [hep-lat]].
- [23] C. Gatttringer, Nucl. Phys. B **850** (2011) 242 doi:10.1016/j.nuclphysb.2011.04.018 [arXiv:1104.2503 [hep-lat]].
- [24] O. Philipsen, EPJ Web Conf. **137** (2017) 03016 doi:10.1051/epjconf/201713703016 [arXiv:1612.03400 [hep-lat]].
- [25] H. Satz, Nucl. Phys. A **642** (1998) 130 doi:10.1016/S0375-9474(98)00508-9 [hep-ph/9805418].